SCATTERING BY A PERFECT ELECTROMAGNETIC CONDUCTING ELLIPTIC CYLINDER

A.-K. Hamid

Department of Electrical and Computer Engineering
University of Sharjah
P. O. Box 27272, Sharjah, United Arab Emirates

F. R. Cooray

CSIRO ICT Centre
P. O. Box 76, Epping, NSW 1710, Australia

Abstract—An exact analytic solution is presented to the problem of scattering of a plane wave from a perfect electromagnetic conducting (PEMC) elliptic cylinder, using the method of separation of variables. The formulation is carried out by expanding the incident as well as the scattered electromagnetic fields in terms of appropriate angular and radial Mathieu functions and a set of expansion coefficients. The incident field expansion coefficients are known, but the scattered field expansion coefficients are unknown. Imposing the boundary conditions at the surface of the elliptic cylinder leads to the determination of the unknown expansion coefficients in closed form. Results are presented as normalized scattering widths for elliptic cylinders of different sizes and PEMC admittances, to show the effects of these on scattering.

1. INTRODUCTION

Research associated with scattering and radiation from impedance loaded objects has been of much interest in the past [1–7]. This in recent years has led to a lot of research on scattering by PEMC objects. A PEMC medium, considered as a generalized form of a perfect electric conducting (PEC) and a perfect magnetic conducting (PMC) medium in which certain linear combinations of electromagnetic fields become extinct [8], is definable by a single real-valued parameter known as the PEMC admittance. A null admittance corresponds to a PMC medium

---

Corresponding author: A.-K. Hamid (akhamid@sharjah.ac.ae).

and an admittance of infinity corresponds to a PEC medium, when the field magnitudes are finite [9].

A PEMC material acts as a perfect reflector of electromagnetic waves, but differs from PEC and PMC materials due to the fact that it produces a reflected wave with cross-polarized field components [10, 11]. This has been demonstrated in the literature recently, by analyzing the scattering of plane waves from an infinitely long PEMC circular cylinder [12, 13], from a PEMC sphere [14, 15], and from a PEMC spheroid [16].

The elliptic cylinder is an object which has been analyzed widely in the literature, as it can produce cylindrical objects of different cross sections when the axial ratio of the ellipse is changed. Furthermore, since the elliptic cylindrical coordinate system is one of the systems in which the wave equation is separable, solutions to problems involving elliptic cylinders can be obtained in closed form. Here, we present for the first time, the analysis pertaining to the scattering of a plane wave of arbitrary polarization and angle of incidence from an infinitely long PEMC elliptic cylinder of arbitrary size and axial ratio. Such a solution is valuable, since it can be used as a benchmark for validating solutions obtained using approximate methods or other numerical methods.

2. FORMULATION

Since a PEMC medium can be considered as the generalization of a PEC and a PMC medium, the boundary conditions to be satisfied at the surface of a PEMC object can be obtained from those to be satisfied at the surfaces of the corresponding PEC and PMC objects as

$$\hat{\mathbf{n}} \times (\mathbf{H} + M\mathbf{E}) = 0, \qquad \hat{\mathbf{n}} \cdot (\mathbf{D} - M\mathbf{B}) = 0 \tag{1}$$

where $\hat{\mathbf{n}}$ is the unit normal to the boundary of the surface, $\mathbf{E}$ and $\mathbf{H}$ are the electric and magnetic fields, respectively, $\mathbf{D}$ and $\mathbf{B}$ are the electric and magnetic flux densities, respectively, and the real-valued scalar parameter M is the PEMC admittance.

Consider a linearly polarized uniform plane electromagnetic wave incident on an infinitely long PEMC elliptic cylinder of semi-major axis length a and semi-minor axis length b, at an angle ϕ_i with respect to the positive x axis of a Cartesian coordinate system located at the centre of the elliptic face, as shown in Fig. 1. The axis of the cylinder is assumed to be along the z axis. From the perspective of the analysis, it is beneficial to define the x and y coordinates of the Cartesian coordinate system, in terms of u and v coordinates of an elliptical coordinate system also located at the centre of the cylinder in the form $x = F \cosh u \cos v$, $y = F \sinh u \sin v$, with F being the
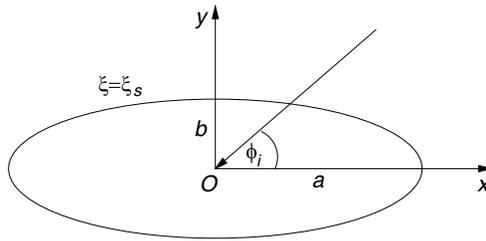
Figure 1. Geometry of the problem.

semi-focal length of the ellipse. A time dependence of $\exp(j\omega t)$ with ω being the angular frequency is assumed throughout the analysis, but suppressed for convenience.

2.1. Transverse Magnetic (TM) Polarization

For a TM polarized incident plane wave, the axial component of the electric field of unit amplitude can be written as $E_z^i = e^{jk\rho\cos(\phi-\phi_i)}$, where $k = 2\pi/\lambda$, with λ being the wavelength in the region exterior to the cylinder, and ρ, ϕ are the polar coordinates. Let the elliptic cylindrical vector wave functions $\mathbf{N}$ and $\mathbf{M} = k^{-1}(\nabla \times \mathbf{N})$ be defined as

$$\mathbf{N}_{qm}^{(i)}(c,\xi,\eta) = R_{qm}^{(i)}(c,\xi)S_{qm}(c,\eta)\hat{\mathbf{z}} \tag{2}$$

$$\mathbf{M}_{qm}^{(i)}(c,\xi,\eta) = \frac{1}{kh}\left[R_{qm}^{(i)}(c,\xi)S'_{qm}(c,\eta)\hat{\mathbf{u}} - R_{qm}^{(i)'}(c,\xi)S_{qm}(c,\eta)\hat{\mathbf{v}}\right] \tag{3}$$

where for $q = e, o$, S_{qm} and $R_{qm}^{(i)}$ are the even and odd angular Mathieu functions and the radial Mathieu functions of the ith kind, both of order m, respectively, $\xi = \cosh u$, $\eta = \cos v$, $c = kF$, $\hat{\boldsymbol{\kappa}}$ denotes a unit vector in the positive κ direction, the primes on S and R denote their respective derivatives with respect to v and u, and $h = F\sqrt{\xi^2 - \eta^2}$.

The incident electric field $\mathbf{E}^i$ can now be expanded in terms of $\mathbf{N}_{qm}^{(1)}$ as

$$\mathbf{E}^i = E_z^i\hat{\mathbf{z}} = \sum_{m=0}^{\infty}A_{em}\mathbf{N}_{em}^{(1)} + \sum_{m=1}^{\infty}A_{om}\mathbf{N}_{om}^{(1)} \tag{4}$$

with the expansion coefficients A_{em} and A_{om} given in [7].

Since the elliptic cylinder is comprised of a PEMC material, the scattered electric field $\mathbf{E}^s$ will contain both co-polarized and cross-polarized components. Thus, it has to be expanded using both $\mathbf{N}_{qm}^{(4)}$

and $\mathbf{M}_{qm}^{(4)}$ as

$$\mathbf{E}^s = \sum_{m=0}^{\infty}\left\{B_{em}\mathbf{N}_{em}^{(4)} + C_{em}\mathbf{M}_{em}^{(4)}\right\} + \sum_{m=1}^{\infty}\left\{B_{om}\mathbf{N}_{om}^{(4)} + C_{om}\mathbf{M}_{om}^{(4)}\right\} \quad (5)$$

where B_{em}, B_{om}, C_{em}, C_{om} are the unknown expansion coefficients. Using Maxwell's equations and referring to (4) and (5), the expansions of the incident and scattered magnetic fields can now be written as

$$\mathbf{H}^i = \frac{j}{Z}\left[\sum_{m=0}^{\infty}A_{em}\mathbf{M}_{em}^{(1)} + \sum_{m=1}^{\infty}A_{om}\mathbf{M}_{om}^{(1)}\right] \quad (6)$$

$$\mathbf{H}^s = \frac{j}{Z}\left[\sum_{m=0}^{\infty}\left\{B_{em}\mathbf{M}_{em}^{(4)} + C_{em}\mathbf{N}_{em}^{(4)}\right\} + \sum_{m=1}^{\infty}\left\{B_{om}\mathbf{M}_{om}^{(4)} + C_{om}\mathbf{N}_{om}^{(4)}\right\}\right] \quad (7)$$

where Z is the wave impedance in the region exterior to the cylinder.

The unknown expansion coefficients can be obtained by imposing the tangential boundary condition in (1) at the surface $\xi = \xi_s$ of the cylinder, which can be expressed mathematically as

$$\left[H_z^i + H_z^s + M\left(E_z^i + E_z^s\right)\right]_{\xi=\xi_s} = 0 \quad (8)$$

$$\left[H_v^i + H_v^s + M\left(E_v^i + E_v^s\right)\right]_{\xi=\xi_s} = 0. \quad (9)$$

Substituting from (4)–(7) in (8)–(9), and applying the orthogonal property of the angular Mathieu functions yield

$$B_{qm} = -\frac{R_{qm}^{(1)'}(c,\xi_s)R_{qm}^{(4)}(c,\xi_s) + Z^2M^2R_{qm}^{(4)'}(c,\xi_s)R_{qm}^{(1)}(c,\xi_s)}{(1+Z^2M^2)R_{qm}^{(4)}(c,\xi_s)R_{qm}^{(4)'}(c,\xi_s)}A_{qm} \quad (10)$$

$$C_{qm} = jMZ\frac{R_{qm}^{(1)}(c,\xi_s)R_{qm}^{(4)'}(c,\xi_s) - R_{qm}^{(4)}(c,\xi_s)R_{qm}^{(1)'}(c,\xi_s)}{(1+Z^2M^2)R_{qm}^{(4)}(c,\xi_s)R_{qm}^{(4)'}(c,\xi_s)}A_{qm} \quad (11)$$

for $q = e, o$. The scattered fields obtained using (10)–(11) in (5) and (7), plus the incident fields, can be shown to satisfy the normal boundary condition in (1), demonstrating the veracity of the solution obtained.

2.2. Transverse Electric (TE) Polarization

The expressions for the incident and scattered electromagnetic fields in this case can be obtained from (4)–(7), using duality. Since the boundary conditions to be satisfied on the surface of the cylinder are

still given by (8)–(9), the unknown expansion coefficients associated with the copolar and cross-polar scattered fields can be obtained from (10) and (11), by interchanging $R_{qm}^{(i)}(c, \xi_s)$ with $R_{qm}^{(i)'}(c, \xi_s)$ for $i = 1, 4$.

3. FAR FIELD

In the limit $\xi \to \infty$, using asymptotic expressions of $R_{qm}^{(4)}(c, \xi)$ and $R_{qm}^{(4)'}(c, \xi)$, E_z^s in the far zone for the TM case can be written as

$$E_z^s = \sqrt{\frac{j}{k\rho}} e^{-jk\rho} \left[\sum_{m=0}^{\infty} j^m B_{em} S_{em}(c, \tau) + \sum_{m=1}^{\infty} j^m B_{om} S_{om}(c, \tau) \right] \quad (12)$$

in which $\tau = \cos\phi$. The expression of E_ϕ^s can be obtained from (12) by changing B_{qm} to C_{qm} and multiplying by j. $H_\phi^s = -E_z^s/Z$ and $H_z^s = E_\phi^s/Z$. The bistatic scattering cross section is defined as

$$\sigma = \lim_{\rho \to \infty} 2\pi\rho \frac{\mathrm{Re}\left[(\mathbf{E}^s \times \mathbf{H}^{s*}) \cdot \hat{\boldsymbol{\rho}}\right]}{\mathrm{Re}\left[(\mathbf{E}^i \times \mathbf{H}^{i*}) \cdot \hat{\boldsymbol{\rho}}\right]} \quad (13)$$

with $\mathrm{Re}[w]$ denoting the real part of a complex number w, the asterisk denoting the complex conjugate, and $\hat{\boldsymbol{\rho}}$ denoting the unit vector in the direction of increasing ρ. After substituting for the scattered fields (in the far zone) and also for the incident fields in (13), we can write an expression for the normalized bistatic scattering width as

$$\frac{\sigma}{\lambda} = \left| \sum_{m=0}^{\infty} j^m B_{em} S_{em}(c, \tau) + \sum_{m=1}^{\infty} j^m B_{om} S_{om}(c, \tau) \right|^2$$

$$+ \left| \sum_{m=0}^{\infty} j^m C_{em} S_{em}(c, \tau) + \sum_{m=1}^{\infty} j^m C_{om} S_{om}(c, \tau) \right|^2. \quad (14)$$

The normalized backscattering width can be obtained by substituting $\phi = \phi_i$ in (14). The normalized bistatic scattering width in the TE case can be expressed in a form similar to (14) too.

4. RESULTS AND CONCLUSION

Results obtained are presented as normalized bistatic and monostatic scattering widths for PEMC elliptic cylinders of different sizes, axial ratios, and PEMC admittances, for TM polarization of the incident wave. For convenience, the PEMC admittance has been expressed in
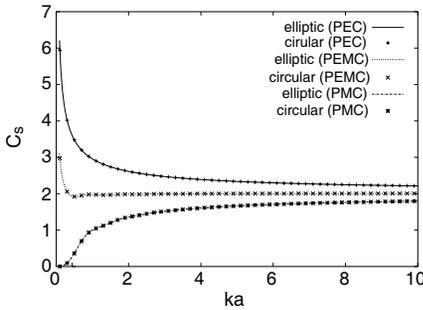
Figure 2. C_s versus ka for an elliptic cylinder of axial ratio ≈ 1 and for a circular cylinder, when $MZ = 0, 1, \infty$.
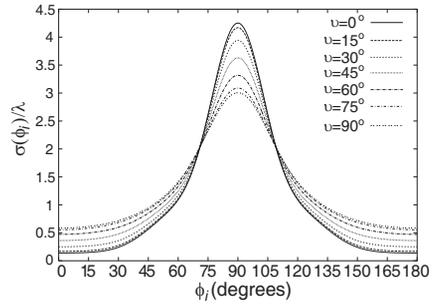
Figure 3. Variation of the normalized backscattering width with the angle of incidence, for elliptic cylinders of axial ratio 2, $ka = \pi$, and different υ.

the dimensionless form $MZ = \tan \upsilon$ [15]. Since results for the TE case with $MZ = \tan \upsilon$ are identical to those for the TM case with $MZ = \tan(90° - \upsilon)$, the results for the TE case have not been presented separately. When calculating the summations in (14), it was sufficient to consider 15 terms to get an accuracy of two significant digits.

To validate the analysis and the software used for calculating the results, we have first computed the normalized backscattering widths for elliptic cylinders of axial ratio 1.001 and semi-major axis lengths $ka = 0.1$ to 10 with normalized PEMC admittances $MZ = 0, 1, \infty$, when they are excited by an arbitrarily incident plane wave. The normalized scattering width C_s in this case is obtained as described in Section 3 of [12]. These results have been compared in Fig. 2 with the corresponding results obtained for a PEMC circular cylinder in [12], and they are in excellent agreement, verifying the accuracy of the analysis and the software used for obtaining the results.

Figure 3 shows the variation of the normalized backscattering width (NBSCW) (σ/λ) for a PEMC elliptic cylinder of axial ratio 2 and semi-major axis length $\lambda/2$ with the angle of incidence, when the PEMC admittance parameter υ changes from $0°$ to $90°$. Here we observe an increase in the NBSCW with υ at a given angle of incidence ϕ_i, when $110° \leq \phi_i \leq 70°$. The change in the NBSCW from $\upsilon = 0°$ to $\upsilon = 90°$ is maximum when $\phi_i = 90°$.

Variations of the normalized bistatic scattering widths (NBSWs) with the scattering angle (ϕ) for the PEMC elliptic cylinders considered in Fig. 3 are shown in Fig. 4, when $\phi_i = 0°$. For $\upsilon = 0°$ and $\upsilon = 15°$, the NBSW is maximum when $\phi = 120°$ and $\phi = 240°$. For all other
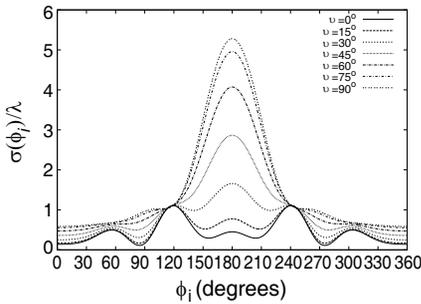
Figure 4. Variation of the normalized bistatic scattering width with the scattering angle for the elliptic cylinders considered in Fig. 3, when they are illuminated by an axially incident plane wave.
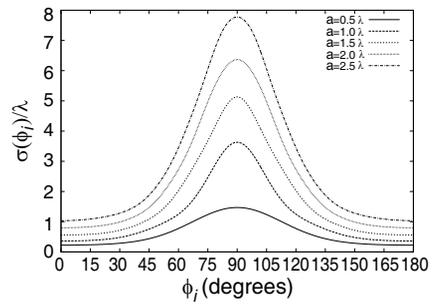
Figure 5. Variation of the normalized backscattering width with the angle of incidence, for elliptic cylinders of axial ratio 2, $\upsilon = 45°$, and different semi-major axis lengths.
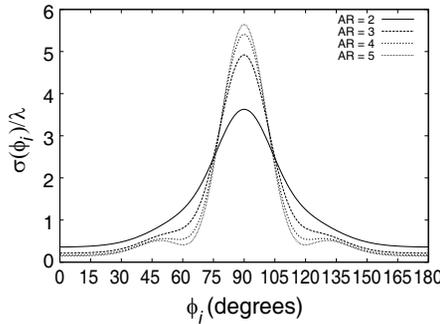

Figure 6. Variation of the normalized backscattering width with the angle of incidence, for elliptic cylinders of $ka = \pi$, $\upsilon = 45°$, and different axial ratios (ARs).

values of υ, it is maximum when $\phi = 180°$ corresponding to forward scattering. The NBSW increases with υ for most values of ϕ, and the increase is more prominent for $150° \leq \phi \leq 210°$.

Figure 5 shows the variation of the NBSCW with ϕ_i for PEMC elliptic cylinders of axial ratio of 2, $\upsilon = 45°$, and 5 different semi-major axis lengths. From these plots we see that the NBSCW increases with the size of the cylinder, since for a larger cylinder the area available for scattering is more. The NBSCW is maximum for all cylinders at broadside incidence corresponding to $\phi_i = 90°$.

Finally, the variation of the NBSCW with ϕ_i for PEMC elliptic cylinders of semi-major axis length $\lambda/2$, $\upsilon = 45°$, and 4 different axial ratios, are shown in Fig. 6. In this case, the patterns become broader as the axial ratio (AR) decreases. All patterns have peaks at $\phi_i = 90°$, with the peaks becoming sharper as the AR increases. For $75° \leq \phi_i \leq 105°$, the NBSCW increases with the AR, but outside this region it decreases as the AR increases from 2 to 5, reaching quite small values close to $\phi_i = 0°$, for AR> 3.

The results obtained in this paper are important, since they can be used as benchmarks to validate similar results obtained using other approximate or numerical methods, and also to get an insight into how the changing of various parameters associated with a PEMC cylinder changes the scattering widths that could be obtained from it.

ACKNOWLEDGMENT

REFERENCES

1. Alexopoulos, N. G., G. A. Tadler, and F. W. Schott, "Scattering from an elliptic cylinder loaded with an active or passive continuously variable surface impedance," *IEEE Trans. Antennas Propag.*, Vol. 22, No. 1, 132–134, 1974.

2. Alexopoulos, N. and G. Tadler, "Electromagnetic scattering and radiation from an elliptic cylinder loaded by continuous and discontinuous surface impedances," *Symp. Digest IEEE AP-S Int. Symp.*, Vol. 12, 303–307, 1974.

3. Alexopoulos, N., P. L. Uslenghi, and G. Tadler, "Antenna beam scanning by active impedance loading," *IEEE Trans. Antenna Propag.*, Vol. 22, No. 5, 722–723, 1974.

4. Alexopoulos, N. G. and G. A. Tadler, "Electromagnetic scattering from an elliptic cylinder loaded by continuous and discontinuous surface impedance," *Journal of Appl. Phys.*, Vol. 46, 1128–1134, 1975.

5. Alexopoulos, N. G., G. A. Tadler, and P. L. E. Uslenghi, "Scattering from spheroidal composite objects," *Journal of Frank. Inst.*, Vol. 309, No. 3, 147–162, 1980.

6. Andreasen, M. G., "Scattering from cylinders with arbitrary surface impedance," *IEEE Trans. Antennas Propag.*, Vol. 53, No. 8, 812–817, 1965.

7. Sebak, A. R., "Scattering from dielectric-coated impedance elliptic cylinder," *IEEE Trans. Antennas Propag.*, Vol. 48, No. 10, 1574–1580, 2000.

8. Lindell, I. V. and A. H. Sihvola, "Perfect electromagnetic conductor," *Journal of Electromagnetic Waves and Applications*, Vol. 19, No. 7, 861–869, 2005.

9. Sihvola, A., I. V. Lindell, and P. Ylä-Oijala, "Scattering properties of PEMC (Perfect Electromagnetic Conducting) materials," *PIERS Proceedings*, 120, Hangzhou, China, Aug. 2005.

10. Lindell, I. V. and A. H. Sihvola, "Perfect electromagnetic conductor (PEMC) in electromagnetics," *PIERS Proceedings*, 119, Hangzhou, China, Aug. 2005.

11. Lindell, I. V. and A. H. Sihvola, "Transformation method for problems involving perfect electromagnetic conductor (PEMC) structures," *IEEE Trans. Antennas Propag.*, Vol. 53, No. 9, 3005–3011, 2005.

12. Ruppin, R., "Scattering of electromagnetic radiation by a perfect electromagnetic conductor cylinder," *Journal of Electromagnetic Waves and Applications*, Vol. 20, No. 13, 1853–1860, 2006.

13. Naqvi, Q. and S. Ahmed, "Electromagnetic scattering from a perfect electromagnetic conductor circular cylinder coated with a metamaterial having negative permittivity and/or permeability," *Optics Comm.*, Vol. 281, No. 23, 5664–5670, 2008.

14. Sihvola, A., P. Ylä-Oijala, and I. V. Lindell, "Bistatic scattering from a PEMC (perfect electromagnetic conducting) sphere: Surface integral equation approach," *Symp. Digest IEEE/ACES Int. Conf. Wireless Comm. Appl. Comp. Electromagnetics*, 317–320, Apr. 2005.

15. Ruppin, R., "Scattering of electromagnetic radiation by a perfect electromagnetic conductor sphere," *Journal of Electromagnetic Waves and Applications*, Vol. 20, No. 12, 1569–1576, 2006.

16. Hamid, A.-K. and F. R. Cooray, "Scattering of electromagnetic waves by a perfect electromagnetic conducting spheroid," *IET Proc. Microwaves Antennas Propag.*, Vol. 2, No. 7, 686–695, 2008.